Tel-Aviv University

Raymond and Beverly Sackler

Faculty of Exact Sciences

School of Physics and Astronomy

Stability of Soft Quasicrystals Composed of Isotropic Particles

Thesis submitted by **Kobi Barkan** in partial fulfillment of the requirements for a M.Sc. degree in physics.

This work was carried out under the supervision of

Prof. Ron Lifshitz and Prof. Haim Diamant.

September 2009

Abstract

The stability of soft-matter quasicrystals is explained by linking between the microscopic description of the system and its coarse-grained free energy. We show, both theoretically and numerically, that the underlying source of the stability is the existence of two natural length-scales and effective three-body interactions, that emerge from the interplay between energy and entropy. We formulate a coarse-grained free-energy functional for a soft-matter system, composed of isotropic particles, which depends on thermodynamical quantities such as temperature, mean density and the critical temperature for the formation of ordered structures from the uniform liquid phase. Using several pair potentials, we study the formation of periodic and quasiperiodic structures displaying various symmetries, and show how one could design the pair potentials to obtain the required structure.

Contents

Acknowledgements

I am grateful to Prof. Ron Lifshitz and Prof. Haim Diamant for not only guiding me in my first steps of academic research, but also for showing me how to focus on the physical issues at hand rather than the technical difficulties. In our frequent talks they provided both instructive questions and striking answers when needed, and I especially appreciate their agreeable manner of doing so.

I would like to thank Prof. Michael Cross, who set me on the right track, even though our single discussion was short. I express my gratitude to my friend and colleague Ely Kovetz for all his support and encouragement.

Last, but not least, I thank my family for their love and moral support, and to my wife Ora—I simply could not have done this without you.

Introduction

In the last few years we have witnessed the exciting experimental discovery of soft matter with nontrivial quasiperiodic long-range order—a new form of matter termed a *soft quasicrystal*. These newly discovered soft quasicrystals provide platforms for the fundamental study of both quasicrystals and of soft matter, and also hold the promise for new applications, such as complete and isotropic photonic band-gap materials, based on self-assembled nanomaterials with unique physical properties that take advantage of the quasiperiodicity. The goal of this work is to explain the source of stability of soft quasicrystals, proposing a theoretical model and providing numerical support. We examine the stability of these soft quasicrystals by linking between the microscopic description of the system and its coarse-grained free energy, and show that the underlying source of stability is the existence of two natural length-scales that emerge from the interaction potential and the existence of effective three-body interactions whose origin is mainly entropic.

The discovery of quasicrystals by Shechtman in 1982 signaled the beginning of a remarkable scientific revolution [1], in which some of the most basic notions of condensed matter physics have undergone a thorough reexamination. In their subsequent publication, Shechtman et al. [2] described the discovery of a new state of matter, that later Levine and Steinhardt [3] named a 'quasicrystal' (QC)—short for quasiperiodic crystal. Shechtman studied Aluminum transition metal alloys and found a solid metal phase with long range order and 5-fold symmetry (icosahedral), but with no translational periodicity. This

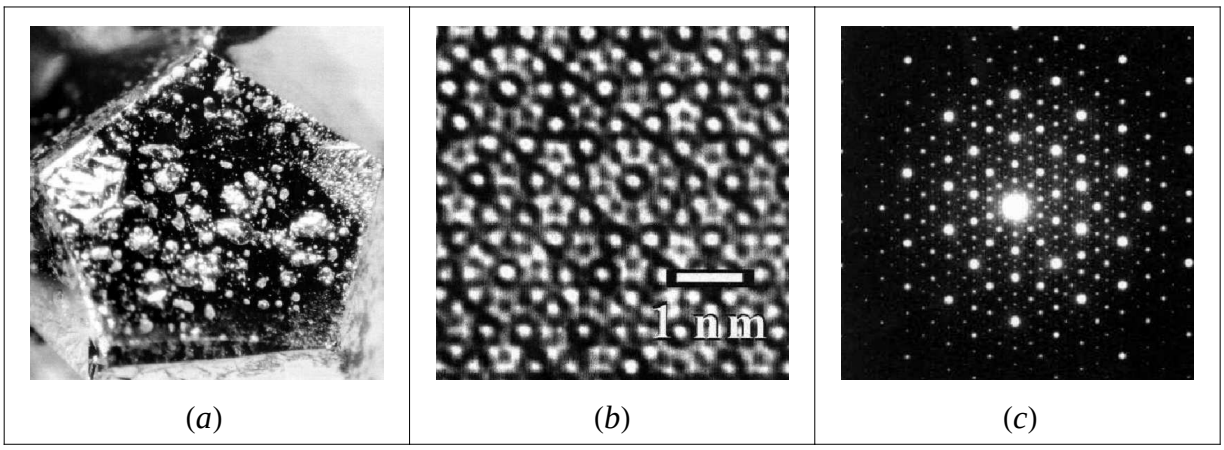

Figure 1: (a) A pentagonal facet of a single grain of a Ho-Mg-Zn QC. (b) Transmission electron microscope image and (c) the diffraction pattern of the 5-fold Dy-Mg-Zn QC. Since for each $\mathbf{k}$ the opposite wave vector $-\mathbf{k}$ also appears, there are 10 Bragg peaks on each circle for a 5-fold QC. All images taken from Ref. [6]

discovery contradicted the old crystallographic paradigm, that defined a crystal as both ordered and periodic. Since 1982, numerous examples of QCs were discovered, most of them binary or ternary metallic alloys with 5-fold or 10-fold (decagonal) symmetries [4, 5], see Fig. 1(a,b).

For both periodic and quasiperiodic crystals, the density $c(\mathbf{r})$ can be expanded as a superposition of plane waves [7],

$$c(\mathbf{r}) = \sum_{\mathbf{k}\in L} \tilde{c}(\mathbf{k}) e^{i\mathbf{k}\cdot\mathbf{r}}, \tag{1}$$

where the set L can be expressed as integral linear combinations of a number D of wave vectors. The Fourier coefficients $\tilde{c}(\mathbf{k})$ are revealed by X-ray diffraction experiments as Bragg peaks as shown in Fig. 1(c). When D is equal to the dimension of space, the crystal is periodic, and its symmetry is limited to 2-, 3-, 4- or 6-fold. When D is larger than the dimension of the space the crystal is quasiperiodic [8–10]. In this case, the set of Bragg peaks is not discrete and k space is dense. However, since any experiment is limited in

sensitivity, it shows only a finite number of wave vectors, producing an "essentially-discrete" diffraction diagram [11].

In spite of the theoretical research in the field of QCs in the past 25 years, several open questions are still being discussed, such as the stability mechanism of QC [5, 12] and the dynamics of phonons and phasons, where the latter are collective energy excitations unique to QCs [13]. Studies of the minimal-energy structures [14,15] and molecular dynamics simulations [16–28] describe stable QCs, assuming various types of pairwise interaction between the particles. In this work we propose a theoretical model that not only demonstrates the stability of single-component QCs, but also give insight to the source of the stability, enabling us to design the pairwise interaction to obtain the required structure.

Recently, as part of the study of soft matter [29], structures with quasiperiodic order were found [30–35]. Behind the name *soft matter* lies a large group of materials including polymer solutions, colloids and liquid crystals that show a certain degree of order [36]. Unlike fluids and solids where either entropy or energy dominates, soft matter is stabilized by an interplay between both thermal excitations and particle interactions. In addition, the length scales are much larger than in the atomic counterparts, and lie in the mesoscopic regime (*i.e.* $1nm - 1\mu m$). These unique features enable complicated phase diagrams with a variety of structures, including liquids, crystals, and liquid crystals [37].

In 2004, Zeng et al. [30–32] discovered a dodecagonal (12-fold) QC phase in a liquid crystal. They used dendrons (tree-like molecules with connectivity 3) that assume a conical shape in solution and self-assemble into spherical micelles, and found that the micelles form a QC structure as shown in Fig. 2. In an independent study, Takano et al. [33, 34] showed that a three-block (ABC) star-polymer system also forms a structure of dodecagonal symmetry. Although there are 3 different polymers, the system can be described by only 2 fields because the overall density is constant and one of the parameters can be scaled out. In this manner, Dotera [38] proposed a mean-field theory with two order parameters to

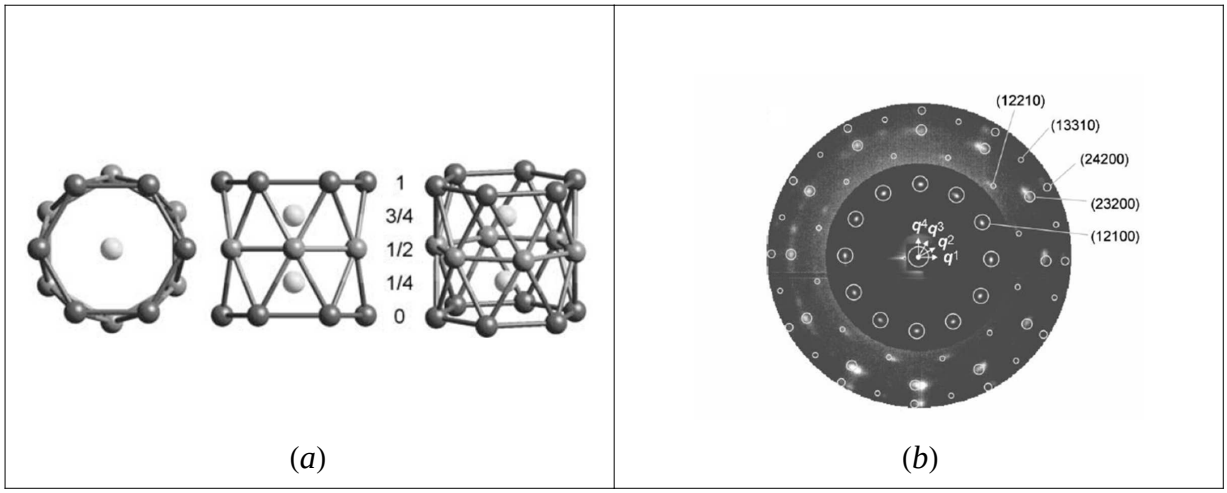

Figure 2: (a) From left to right, top, side and isometric views of a cluster of spheres with 12-fold symmetry. (b) Experimental X-ray diffraction pattern of the liquid QC showing 12 Bragg peaks on the first circle. Images describing the work of Zeng et al. [30].

explain the stability of the three-block star-polymer QCs. Recently, Percec et al. [35] have provided yet another example of dodecagonal soft-matter QCs, which like the first one, are composed of spherical micelles. The purpose of this work is to develop a model for soft-matter QCs relying on a microscopic description of a single-component system composed of isotropic particles.

The significance of the discovery of quasiperiodic structures in soft matter has several aspects. First, in these soft-matter systems the particles are in fact supramolocular aggregates of thousands of atoms in the form of micelles or star polymers. These structures are 100 times larger than regular metal atoms that are the building blocks of metal alloy crystals and QCs. Second, because the quasiperiodic order resides in a plane, the third axis shows a regular periodic order of planes of QCs and therefore one is left with an effective two-dimensional problem rather than a three-dimensional one. Third, to this date, soft quasicrystals have been observed only with dodecagonal point-group symmetry, in place of the 5-, 8- or 10-fold symmetries encountered before in solid-state systems, suggesting that

their source of stability is likely to be different from their solid-state siblings. Finally, the liquid is composed of only one type of micelles, instead of compounds of two or three types of atoms for metal based QCs. This means that the interaction between pairs of particles is determined by a single pair potential, whereas in metals one has to consider several different pair interactions for all the combinations of the different atoms. We will show that these exceptional properties of soft-matter QCs provide a relatively simple physical system, for which the stability of the quasiperiodic pattern can be accounted for.

We draw our inspiration from the work of Lifshitz and Petrich [39], who studied the stability of systems with quasiperiodic order via a free energy that features two different length scales and three-body interactions. Motivated by experiments with parametrically-excited surface waves (Faraday waves), exhibiting dodecagonal (12-fold) quasiperiodic order [40–42], Lifshitz and Petrich developed a model describing the pattern-forming dynamics of a two-dimensional field in which two length scales undergo a simultaneous instability. The dodecagonal quasiperiodic order is energetically preferred for a certain ratio between the two wavelengths, and when the three-body interactions are sufficiently strong compared with the pairwise interactions. This relates to soft QCs, as Lifshitz and Diamant [43] discuss, because the soft-matter experimental systems that show quasiperiodic order are expected to possess two length scales and relatively strong three-body interactions. In this work we prove their conjecture and show how one can tune the pairwise interaction to stabilize the required structure. In Chapter 1 we compare the Lifshitz and Petrich free energy with a mean-field free energy for a single component liquid with pairwise isotropic interactions, and find the requirements on the experimental parameters needed to obtain a thermodynamically stable dodecagonal QC. In Chapter 2 we give several examples for interactions that fulfill these requirements. We present the results of a numerical simulations that show the formation of a dodecagonal QC for such conditions in Chapter 3 and conclude with some final remarks and ideas for future research.

Chapter 1

Theoretical Model

1.1 The Lifshitz-Petrich equation

The inspiration to this work comes from the free energy proposed by Lifshitz and Petrich (LP) [39], that was motivated by the existence of two-dimensional dodecagonal quasiperiodic patterns in Faraday waves [40–42]. They started from the Swift-Hohenberg equation [44],

$$\partial_t \rho = \varepsilon \rho - \left(\nabla^2 + 1\right)^2 \rho - \rho^3, \tag{1.1}$$

where ρ is the deviation from the mean value of the field describing the two-dimensional problem at hand, and the gradient term prefers one length scale that is set here to 1. The Swift-Hohenberg equation is often used to model a supercritical instability and pattern formation in various systems. It is variational, *i.e.* it can be written as

$$\partial_t \rho = -\frac{\delta \mathcal{F}}{\delta \rho}, \tag{1.2}$$

where $\mathcal{F}$ is an effective free energy,

$$\mathcal{F}_{SH} = \int d\mathbf{r} \left[-\frac{1}{2}\varepsilon\rho(\mathbf{r})^2 + \frac{1}{2}\left[(\nabla^2+1)\rho(\mathbf{r})\right]^2 + \frac{1}{4}\rho(\mathbf{r})^4 \right]. \tag{1.3}$$

Thus, a steady-state solution of the Swift-Hohenberg equation (1.1) minimizes the effective free energy (1.3). LP suggested a modified expression,

$$\mathcal{F} = \int d\mathbf{r} \left[-\frac{1}{2}\varepsilon\rho(\mathbf{r})^2 + \frac{1}{2}c\left[(\nabla^2+1)(\nabla^2+q^2)\rho(\mathbf{r})\right]^2 - \frac{1}{3}\alpha\rho(\mathbf{r})^3 + \frac{1}{4}\rho(\mathbf{r})^4 \right], \tag{1.4}$$

where they incorporated two features from the Faraday wave experimental system: effective three-body interactions that are controlled by the parameter α, and the existence of two dominant wavelengths whose ratio is q. The selection of the wavelengths is controlled by the gradient terms and its strength by the parameter c. The forth power of ρ stabilizes the system by providing a lower bound for the free energy. The coefficient α of the three-body interaction can be scaled out, and by denoting $\varepsilon^* = \frac{\varepsilon}{\alpha^2}$ and $c^* = \frac{c}{\alpha^2}$, one obtains the Lifshitz-Petrich scaled free energy [39]

$$\mathcal{F}_{LP} = \int d\mathbf{r} \left[-\frac{1}{2}\varepsilon^*\rho(\mathbf{r})^2 + \frac{1}{2}c^*\left[(\nabla^2+1)(\nabla^2+q^2)\rho(\mathbf{r})\right]^2 - \frac{1}{3}\rho(\mathbf{r})^3 + \frac{1}{4}\rho(\mathbf{r})^4 \right]. \tag{1.5}$$

The gradient terms have zero contribution to the LP free energy for wavelengths whose magnitude is either 1 or q. If the parameter c^* is sufficiently large, the system energetically selects wavelengths at these magnitudes. Assuming a perfect selection, LP wrote the free energy in Fourier space as

$$\mathcal{F}_{LP} = -\frac{\varepsilon^*}{2}\sum_{|\mathbf{k}|=1,q}\rho_{\mathbf{k}}\rho_{-\mathbf{k}} - \frac{1}{3}\sum_{|\mathbf{k}_i|=1,q}\rho_{\mathbf{k}_1}\rho_{\mathbf{k}_2}\rho_{-\mathbf{k}_1-\mathbf{k}_2} + \frac{1}{4}\sum_{|\mathbf{k}_i|=1,q}\rho_{\mathbf{k}_1}\rho_{\mathbf{k}_2}\rho_{\mathbf{k}_3}\rho_{-\mathbf{k}_1-\mathbf{k}_2-\mathbf{k}_3}, \tag{1.6}$$

where the summation is restricted to wave-vectors whose magnitude is either 1 or q, *i.e.* ly-

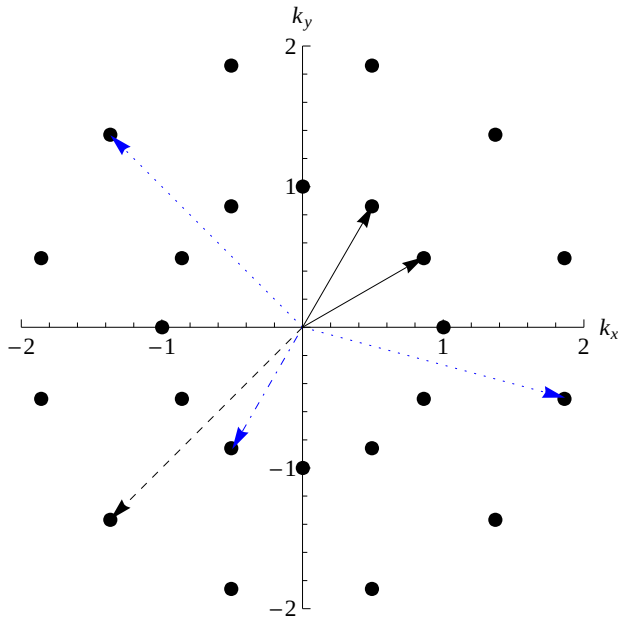

Figure 1.1: Wave-vectors lying on two rings in a two-dimensional Fourier space. The ratio between the radii of the rings is chosen so that the sum of two adjacent wave-vectors on the first ring (solid lines) cancels a wave-vector on the second ring (dashed line). Note that at the same time the sum of two wave-vectors on the second ring (dotted lines) cancels a wave-vector on the first ring (dashed-dotted line). Here $q = 2\cos\left(\frac{\pi}{12}\right) = \sqrt{2+\sqrt{3}}$ in order to prefer 12-fold symmetry.

ing on one of two rings with radii ratio q in the two-dimensional Fourier space as shown in Fig. 1.1. The system chooses the overall phases of $\rho_{\mathbf{k}_i}$ so that the second term in Eq. (1.6) lowers the free energy. Note that the second term is a sum over all triplets of wave-vectors whose vector sum is zero, and thus, three-body interactions can lower the free energy.

For N-fold symmetry, there are N Bragg peaks on each ring. The lowest free energy is obtained when the ratio q between the rings is such that the sum of two wave-vectors on one ring and a third wave-vector from the second ring is zero, as shown in Fig. 1.1. This means that for N-fold symmetry the ratio q should be equal to the magnitude of the vector sum of two unit vectors separated by an angle of $\frac{2\pi}{N}$, *i.e.*

$$q = 2\cos\left(\frac{\pi}{N}\right). \tag{1.7}$$

Note that for any N-fold symmetry the value of q is between 1 and 2.

Using standard methods LP [39] calculated the free energy for several patterns and found that when the ratio q is chosen to prefer 12-fold symmetry, the resulting stable pattern depends upon the value of the parameter ε^*. An N-fold symmetry is stable for a range of values

$$\varepsilon_{min}^{*(N)} < \varepsilon^* = \frac{\varepsilon}{\alpha^2} < \varepsilon_{max}^{*(N)}, \tag{1.8}$$

where a dodecagonal pattern is stable with $\varepsilon_{min}^{*(12)} = 0$ and $\varepsilon_{max}^{*(12)} \simeq 0.08776$. This condition implies that the three-body interactions, that are controlled by the parameter α, should be sufficiently strong compared with the pairwise interactions, controlled by the parameter ε. If the interactions are weaker, a 6-fold pattern is obtained for ε^* between $\varepsilon_{min}^{*(6)} \simeq 0.08776$ and $\varepsilon_{max}^{*(6)} \simeq 1.91313$, and a 2-fold pattern whenever ε^* is larger than $\varepsilon_{min}^{*(2)} \simeq 1.91313$. 2-fold, 4-fold and 6-fold symmetries are obtained when the ratio q is selected according to Eq. (1.7), possibly with superstructure ordering. When q is selected to prefer 8-fold or 10-fold patterns, the system nevertheless prefers a 6-fold periodic pattern with 6 wave-vectors lying on one ring in Fourier space. Thus, 8-fold and 10-fold patterns are not found to be stable with the LP free energy.

To sum up, Lifshitz and Petrich found that dodecagonal QCs are stable when three-body interactions are sufficiently strong and two length scales exist. When the value of the ratio q prefers 12-fold symmetry (1.7), a dodecagonal QC is stable for a range of values of the free energy parameters given in Eq. (1.8). Their work provides us with valuable insight to the stability of QCs in soft-matter systems, where complicated molecular structures give rise to two length scales, and where three-body interactions may be strong, as we show in the following section.

1.2 A coarse-grained free energy for pairwise interactions

We take the partition function of a system of discrete identical particles with a pairwise interaction, denoted by $U(|\mathbf{r}-\mathbf{r}'|)$, and coarse-grain it to obtain a free-energy functional of a continuous density. The Appendix describes a rigorous coarse-graining scheme that can be later extended to include higher-order correlations, yet for our current purposes it suffices to use the leading mean-field result (A.21), which we reproduce here

$$\mathcal{F} = \frac{1}{2}\int d\mathbf{r}d\mathbf{r}' c(\mathbf{r})U(|\mathbf{r}-\mathbf{r}'|)c(\mathbf{r}') + k_BT\int d\mathbf{r}\left(c(\mathbf{r})\ln\frac{c(\mathbf{r})}{Z_0\zeta} - c(\mathbf{r})\right), \tag{1.9}$$

where c is the density, $\zeta = e^{\beta\mu}$ is the fugacity, and μ is the chemical potential. We denote $Z_0 = e^{\frac{1}{2}\beta U(0)}/\Lambda^d$, where $\beta = 1/k_BT$ is the inverse temperature, $\Lambda = h/\sqrt{2\pi m k_BT}$ is the thermal de Broglie wavelength, and d is the dimensionality. Note that the second term in this free energy is just the entropy of an ideal gas.

We want to expand the free energy as a power series of the deviations δc from the average density an its gradients, and then cut off the expansion to obtain an expression similar to the LP free energy (1.5). Since the free energy (1.9) is formulated in the grand-canonical ensemble, the mean density is given by the equation

$$0 = \frac{\delta\mathcal{F}}{\delta c} = \bar{c}\int d\mathbf{r}' U(|\mathbf{r}-\mathbf{r}'|) + k_BT\ln\frac{\bar{c}}{Z_0\zeta} = \bar{c}\bar{U}V + k_BT\ln\frac{\bar{c}}{Z_0\zeta}, \tag{1.10}$$

where V is the volume of the system, and $\bar{U} = \frac{1}{V}\int d\mathbf{r}U(\mathbf{r})$ is the volume-average of the pairwise interaction. We find the average density to be

$$\bar{c} = Z_0\zeta\exp\left(-\frac{\bar{c}\bar{U}V}{k_BT}\right) = Z_0\zeta\exp\left(-\frac{N\bar{U}}{k_BT}\right), \tag{1.11}$$

where $N = V\bar{c}$ is the number of particles.

We expand the free energy (1.9), in density variations δc around $\bar{c}$

$$\begin{aligned}\mathcal{F} &= \mathcal{F}_0 + \sum_{n=2}^{\infty} \frac{(\delta c(\mathbf{r}))^n}{n!} \frac{\delta^n \mathcal{F}}{\delta c(\mathbf{r})^n}\bigg|_{c(\mathbf{r})=\bar{c}} \\ &= \mathcal{F}_0 + \frac{1}{2}\int d\mathbf{r}d\mathbf{r}'\delta c(\mathbf{r})U(|\mathbf{r}-\mathbf{r}'|)\delta c(\mathbf{r}') \\ &\quad + k_BT\int d\mathbf{r}\sum_{n=2}^{\infty}\frac{(\delta c(\mathbf{r}))^n}{n!}\frac{\partial^n}{\partial c(\mathbf{r})^n}\left(c(\mathbf{r})\ln\frac{c(\mathbf{r})}{Z_0\zeta} - c(\mathbf{r})\right)\bigg|_{c(\mathbf{r})=\bar{c}}, \end{aligned} \tag{1.12}$$

and cut off the sum at the 4^{th} order of δc like the LP free energy to obtain, up to a constant,

$$\mathcal{F} \approx \frac{1}{2}\int d\mathbf{r}d\mathbf{r}'\delta c(\mathbf{r})U(|\mathbf{r}-\mathbf{r}'|)\delta c(\mathbf{r}') + k_BT\int d\mathbf{r}\left[\frac{1}{2}\frac{\delta c(\mathbf{r})^2}{\bar{c}} - \frac{1}{3}\frac{\delta c(\mathbf{r})^3}{2\bar{c}^2} + \frac{1}{4}\frac{\delta c(\mathbf{r})^4}{3\bar{c}^3}\right]. \tag{1.13}$$

Such an expansion in powers of density variations is expected to be particularly appropriate for soft matter, where density gradients are much smaller than in atomic or molecular systems.

We now turn to Fourier space in order to rewrite the energy term using Parseval's identity. Taking the Fourier transform of the pair potential

$$\tilde{U}(\mathbf{k}) \equiv \int d\mathbf{r}U(\mathbf{r})e^{-i\mathbf{k}\cdot\mathbf{r}}, \tag{1.14}$$

and the Fourier transform of the density variations

$$\delta\tilde{c}(\mathbf{k}) \equiv \int d\mathbf{r}\delta c(\mathbf{r})e^{-i\mathbf{k}\cdot\mathbf{r}}, \tag{1.15}$$

we rewrite the energy term (denoted by $\mathcal{F}_U$) as

$$\begin{aligned}
\mathcal{F}_U &= \frac{1}{2}\int d\mathbf{r}d\mathbf{r}'\delta c(\mathbf{r})U(|\mathbf{r}-\mathbf{r}'|)\delta c(\mathbf{r}') \\
&= \frac{1}{2}\int d\mathbf{r}d\mathbf{r}'\delta c(\mathbf{r})\left(\int \frac{d\mathbf{k}}{(2\pi)^d}\tilde{U}(\mathbf{k})e^{i\mathbf{k}\cdot(\mathbf{r}-\mathbf{r}')}\right)\delta c(\mathbf{r}') \\
&= \frac{1}{2}\int \frac{d\mathbf{k}}{(2\pi)^d}\tilde{U}(\mathbf{k})\int d\mathbf{r}\delta c(\mathbf{r})e^{i\mathbf{k}\cdot\mathbf{r}}\int d\mathbf{r}'\delta c(\mathbf{r}')e^{-i\mathbf{k}\cdot\mathbf{r}'} \\
&= \frac{1}{2}\int \frac{d\mathbf{k}}{(2\pi)^d}\tilde{U}(\mathbf{k})\delta\tilde{c}(-\mathbf{k})\delta\tilde{c}(\mathbf{k}),
\end{aligned} \tag{1.16}$$

where d is the dimensionality. Next, we expand the Fourier transform of the pair potential in powers of $\mathbf{k}$. The pair potential is assumed isotropic in real space, *i.e.* $U(\mathbf{r}) = U(|\mathbf{r}|)$, and therefore its Fourier transform is isotropic in momentum space, *i.e.* $\tilde{U}(\mathbf{k}) = \tilde{U}(|\mathbf{k}|)$. Hence, we can expand the pair potential in powers of $\mathbf{k}\cdot\mathbf{k} = k^2$,

$$\tilde{U}(\mathbf{k}) = \sum_{n=0}^{\infty} a_{2n}k^{2n}, \tag{1.17}$$

and obtain

$$\begin{aligned}
\mathcal{F}_U &= \frac{1}{2}\int \frac{d\mathbf{k}}{(2\pi)^d}\sum_{n=0}^{\infty} a_{2n}k^{2n}\delta\tilde{c}(-\mathbf{k})\delta\tilde{c}(\mathbf{k}) \\
&= \frac{1}{2}\int \frac{d\mathbf{k}}{(2\pi)^d}\sum_{n=0}^{\infty} a_{2n}\left[k^n\delta\tilde{c}(-\mathbf{k})\right]\left[k^n\delta\tilde{c}(\mathbf{k})\right].
\end{aligned} \tag{1.18}$$

The next step is to replace the powers of k with gradients of δc. When we transform

back to real space, each multiplication by k is replaced by a gradient, and we are left with

$$\begin{aligned}
\mathcal{F}_U &= \frac{1}{2}\int \frac{d\mathbf{k}}{(2\pi)^d}\sum_{n=0}^{\infty} a_{2n}\int d\mathbf{r}(-i)^n\nabla^n\delta c(\mathbf{r})e^{i\mathbf{k}\cdot\mathbf{r}}\int d\mathbf{r}'(i)^n\nabla'^n\delta c(\mathbf{r}')e^{-i\mathbf{k}\cdot\mathbf{r}'} \\
&= \frac{1}{2}\int d\mathbf{r}d\mathbf{r}'\sum_{n=0}^{\infty} a_{2n}\nabla^n\delta c(\mathbf{r})\nabla'^n\delta c(\mathbf{r}')\int \frac{d\mathbf{k}}{(2\pi)^d}e^{-i\mathbf{k}\cdot(\mathbf{r}'-\mathbf{r})} \\
&= \frac{1}{2}\int d\mathbf{r}d\mathbf{r}'\sum_{n=0}^{\infty} a_{2n}\delta\left(\mathbf{r}'-\mathbf{r}\right)\nabla^n\delta c(\mathbf{r})\nabla'^n\delta c(\mathbf{r}') \\
&= \frac{1}{2}\int d\mathbf{r}\sum_{n=0}^{\infty} a_{2n}\left[\nabla^n\delta c(\mathbf{r})\right]^2 . \qquad (1.19)
\end{aligned}$$

The derivative ∇^n is understood as $(\nabla^2)^m$ for even n, and as $(\nabla^2)^m\nabla$ for odd n. Such an expansion in gradients is appropriate for soft matter, where the length scale of the density variations is large. Substituting the last expression for the potential energy into the free energy, Eq. (1.13), we have

$$\mathcal{F} = \int d\mathbf{r}\left[\frac{1}{2}\sum_{n=0}^{\infty} a_{2n}\left[\nabla^n\delta c(\mathbf{r})\right]^2 + k_BT\left(\frac{1}{2}\frac{\delta c(\mathbf{r})^2}{\bar{c}} - \frac{1}{3}\frac{\delta c(\mathbf{r})^3}{2\bar{c}^2} + \frac{1}{4}\frac{\delta c(\mathbf{r})^4}{3\bar{c}^3}\right)\right], \qquad (1.20)$$

which is of the form of the LP free energy, Eq. (1.5).

The final step is to show how the critical temperature for crystallization is determined. We denote the minimum of the Fourier transform of the pair potential $\tilde{U}(\mathbf{k})$ by $\tilde{U}_{min}$, subtract this contribution from the energy term and add it to the entropy term to obtain

$$\begin{aligned}
\mathcal{F} = \int d\mathbf{r}\Bigg[&\frac{1}{2}(a_0-\tilde{U}_{min})\delta c(\mathbf{r})^2 + \frac{1}{2}\sum_{n=1}^{\infty} a_{2n}\left[\nabla^n\delta c(\mathbf{r})\right]^2 \\
&+ k_BT\left(\frac{\delta c(\mathbf{r})^2}{2}\left(\frac{\tilde{U}_{min}}{k_BT}+\frac{1}{\bar{c}}\right) - \frac{1}{3}\frac{\delta c(\mathbf{r})^3}{2\bar{c}^2} + \frac{1}{4}\frac{\delta c(\mathbf{r})^4}{3\bar{c}^3}\right)\Bigg]. \qquad (1.21)
\end{aligned}$$

For the sake of simplicity, we re-define the expansion coefficients $\{a_{2n}\}$ to compensate for

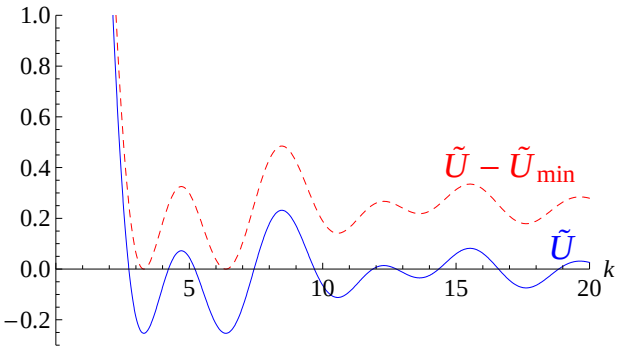

Figure 1.2: The Fourier transform of the pair potential $\tilde{U}(\mathbf{k})$ (solid curve) and its shifted form (dashed curve) where the value of the minima is exactly zero.

$\tilde{U}_{min}$,

$$\tilde{U}(\mathbf{k}) - \tilde{U}_{min} = \sum_{n=0}^{\infty} \tilde{a}_{2n} k^{2n}, \tag{1.22}$$

as shown in Fig. 1.2, and obtain

$$\mathcal{F} = \int d\mathbf{r} \left[\frac{1}{2} \sum_{n=0}^{\infty} \tilde{a}_{2n} \left[\nabla^n \delta c(\mathbf{r}) \right]^2 + k_B T \left(\frac{\delta c(\mathbf{r})^2}{2} \left(\frac{\tilde{U}_{min}}{k_B T} + \frac{1}{\bar{c}} \right) - \frac{1}{3} \frac{\delta c(\mathbf{r})^3}{2\bar{c}^2} + \frac{1}{4} \frac{\delta c(\mathbf{r})^4}{3\bar{c}^3} \right) \right]. \tag{1.23}$$

The uniform state becomes unstable when the quadratic term changes sign from positive to negative. Because the gradient term is zero at the minima of $\tilde{U}(\mathbf{k})$, the sign of the coefficient of the quadratic term is determined by the term $\tilde{U}_{min} + k_B T/\bar{c}$, as shown in Fig. 1.3. Therefore, we identify the critical temperature as

$$k_B T_c \equiv -\tilde{U}_{min} \bar{c}. \tag{1.24}$$

Note that the critical temperature is thus defined only if $\tilde{U}_{min} < 0$. We divide the free

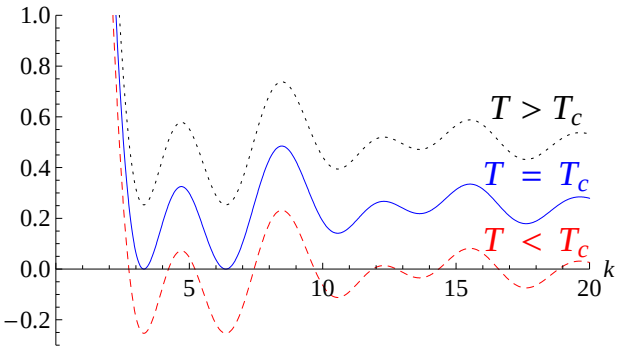

Figure 1.3: Solid curve—the coefficient of $\delta c(\mathbf{r})^2$ at the critical temperature T_c, where the value of the two minima is exactly zero. Dotted curve—above T_c, where the coefficient is positive for all k-values. Dashed curve—below T_c, where regions around the minima have a negative sign.

energy by the critical temperature, to obtain the familiar form

$$\frac{\mathcal{F}}{k_B T_c} = \int d\mathbf{r} \left[\frac{1}{2k_B T_c} \sum_{n=0}^{\infty} \tilde{a}_{2n} \left[\nabla^n \delta c(\mathbf{r})\right]^2 + \frac{\delta c(\mathbf{r})^2}{2\bar{c}} \left(\frac{T - T_c}{T_c}\right) - \frac{1}{3}\frac{T}{T_c}\frac{\delta c(\mathbf{r})^3}{2\bar{c}^2} + \frac{1}{4}\frac{T}{T_c}\frac{\delta c(\mathbf{r})^4}{3\bar{c}^3} \right]. \tag{1.25}$$

Using a dimensionless deviation from the mean density defined as

$$\rho(\mathbf{r}) \equiv \frac{2}{3}\frac{\delta c(\mathbf{r})}{\bar{c}}, \tag{1.26}$$

we rescale the free energy and obtain

$$\mathcal{F}_{isotropic} \equiv \mathcal{F}\frac{2^4}{3^3 k_B T_c \bar{c}} = \int d\mathbf{r} \left[\frac{2^3}{3^3 k_B T_c \bar{c}} \sum_{n=0}^{\infty} \tilde{a}_{2n} \left[\nabla^n \rho(\mathbf{r})\right]^2 + \frac{4}{3}\left(\frac{T - T_c}{T_c}\right)\frac{\rho(\mathbf{r})^2}{2} - \frac{T}{T_c}\frac{\rho(\mathbf{r})^3}{3} + \frac{T}{T_c}\frac{\rho(\mathbf{r})^4}{4} \right]. \tag{1.27}$$

Note that since T is assumed close to T_c, the factor of T/T_c is of order 1. In fact, we do not have to calculate the coefficients of the expansion $\tilde{a}_{2n}$ (1.22), but we give them here (1.27)

explicitly in order to show the similarity between the pair potential contribution and LP's wavelength selection term (1.5). We could, instead, express the free energy of the identical isotropic particles using the actual Fourier transformed pair potential $\tilde{U}(\mathbf{k})$, rather than its power expansion, and obtain the main result of this section

$$\mathcal{F}_{isotropic} = \int \frac{d\mathbf{k}}{(2\pi)^d} \frac{2^3}{3^3 k_B T_c \bar{c}} \left(\tilde{U}(\mathbf{k}) - \tilde{U}_{min}\right) \tilde{\rho}(-\mathbf{k})\tilde{\rho}(\mathbf{k}) + \int d\mathbf{r} \left[\frac{4}{3}\left(\frac{T-T_c}{T_c}\right)\frac{\rho(\mathbf{r})^2}{2} - \frac{T}{T_c}\frac{\rho(\mathbf{r})^3}{3} + \frac{T}{T_c}\frac{\rho(\mathbf{r})^4}{4}\right]. \tag{1.28}$$

In order to obtain 12-fold symmetry, we first have to satisfy the condition concerning the ratio q between the minima, stated in Eq. (1.7). We show how the selection of q is made possible in the next chapter. Overall, the physical parameters that control the free energy are $\bar{c}, T$ and $\tilde{U}_{min}$. We compare our result with the LP free energy $\mathcal{F}_{LP}$ (1.5), and find that the range of values of the parameter ε^*, given by Eq. (1.8), corresponds to a range of values for the temperature

$$1 - \frac{3}{4}\varepsilon^{*(N)}_{max} < \frac{T}{T_c} < 1 - \frac{3}{4}\varepsilon^{*(N)}_{min}. \tag{1.29}$$

When q is set to prefer 12-fold patterns, we find that while a structure with 12-fold symmetry is stable for

$$0.9382 \lesssim \frac{T}{T_c} < 1, \tag{1.30}$$

and a structure with 6-fold symmetry is stable for

$$0 < \frac{T}{T_c} \lesssim 0.9382, \tag{1.31}$$

a 2-fold pattern, unlike the LP case, is not stable in this case because it will require a negative temperature. In order to find the region in parameter space for which the

dodecagonal phase is stable, we use the definition of the critical temperature (1.24) and find the requirement

$$0.9382 \lesssim \frac{k_B T}{-\tilde{U}_{min}\bar{c}} < 1, \tag{1.32}$$

where $\tilde{U}_{min}$ is assumed negative.

To conclude, we have been able to derive from a microscopic partition function a coarse-grained mean-field free energy similar to the LP free energy. We have subsequently found the corresponding conditions where the LP results apply, namely, the stability of different N-fold patterns. The expansion of the entropy term in powers of ρ is sufficient to provide an effective three-body interaction term ρ^3, which is essential for the stability of quasiperiodic symmetries in the LP description. The expansion of the energy term in gradients of ρ effectively selects two wavelengths with a ratio q, as discussed in detail in the next chapter.

Chapter 2

Isotropic Pair Potentials with Two Length Scales

This chapter is devoted to presenting several two-dimensional isotropic pair potentials that enable stabilizing various symmetries, and specifically, the 12-fold symmetry that was observed in soft materials. The pair potential contribution to the free energy (1.28) corresponds to the quadratic term of the LP free energy $\mathcal{F}_{LP}$ (1.5),

$$\mathcal{F}_2\{\rho(\mathbf{r})\} = -\frac{1}{2}\varepsilon^*\rho(\mathbf{r})^2 + \frac{1}{2}c^*\left[(\nabla^2+1)(\nabla^2+q^2)\rho(\mathbf{r})\right]^2, \tag{2.1}$$

which becomes a polynomial in k^2 when expressed in Fourier space

$$\begin{aligned}\tilde{\mathcal{F}}_2\{\rho_{\mathbf{k}}\} &= -\frac{1}{2}\varepsilon^*|\rho_{\mathbf{k}}|^2 + \frac{1}{2}c^*\left|(-k^2+1)(-k^2+q^2)\rho_{\mathbf{k}}\right|^2 \\ &= \frac{c^*}{2}\left[k^8 - 2k^6(q^2+1) + k^4(q^4+4q^2+1) - 2k^2(q^4+q^2) + (1-\frac{\varepsilon^*}{c^*})q^4\right]|\rho_{\mathbf{k}}|^2.\end{aligned} \tag{2.2}$$

As shown in Fig. 2.1, the polynomial is constructed so that it has two equal-height minima, one at $k=1$, and the second at $k=q$. Wavelengths that match these minima are selected

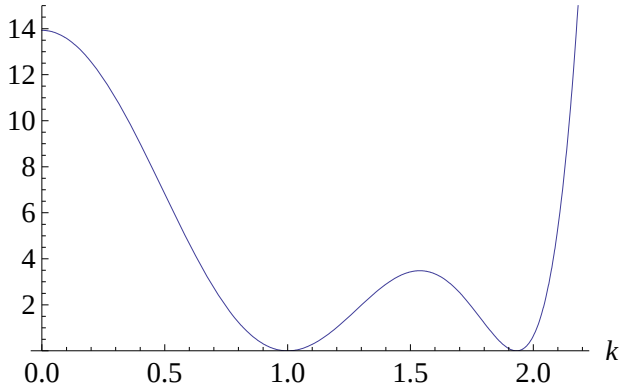

Figure 2.1: LP's wavelength selection term in Fourier space where $c^* = 2$, $\varepsilon^* = 0$ and $q = 2\cos(\frac{\pi}{12})$, see Eq. (2.2)

because they minimize the free energy. However, for the Fourier transform of a pair potential $\tilde{U}(\mathbf{k})$, we have to tune the parameters of the potential so that the heights of the minima are equal. This is because a sufficiently large difference between the heights of the minima, compared with the temperature, will cause the system to choose the lower minimum, and the second length scale, crucial for the stability of QCs, will be lost. Therefore, $\tilde{U}(\mathbf{k})$ has to have two minima with a minimal difference between their heights.

In addition, as we discussed in section 1.1, in order to stabilize a structure with N-fold symmetry in two dimensions, the ratio q between the minima has to satisfy the geometrical condition (1.7). Consequently, the two-dimensional pair potential has to have at least two length scales so that in Fourier space both the height of and the ratio between the minima can be tuned to stabilize the desired structure. Alternatively, since we have two conditions, we must have at least two independent parameters in the pair potential to obtain a solution. While many different isotropic potentials, with at least two length scales, were shown to stabilize quasicrystals [14–28], here we provide a theoretical model that enables one to tune the parameters of the pairwise interaction, by analyzing its Fourier transform, in order to obtain the desired structure.

We focus here on the simple case of isotropic particles in two-dimensions, interacting

via circularly symmetric potentials (*i.e.* $U(\mathbf{r}) = U(r)$). In the study of Zeng et al. [30–32], spherical micelles were the building blocks of their 12-fold QC. These micelles are composed of conical shaped dendrimers joined at the head, and can be described as having a harder core and a softer repulsion at greater distances. Therefore, we start by characterizing the pair potential between such micelles using a box-like pair potential, and then move on to more realistic interactions.

2.1 Piecewise constant pair potential—two boxes

Let us start with the simplest potential we can use to describe the interaction between the micelles—a piecewise constant potential with two length scales

$$U(r) = \begin{cases} 1 & 0 < r < 1 \\ u & 1 < r < R \\ 0 & R < r < \infty, \end{cases} \tag{2.3}$$

where r is the distance between the two particles. It contains a repulsive core, whose strength and radius are normalized to unity, and an additional repulsive shoulder with strength u extending to a radius R, the two free parameters, as shown in Fig. 2.2(a).

The Fourier transform of a circularly symmetric function in two dimensions is the so-called Hankel transform

$$\begin{aligned} \tilde{U}(k) &= \int d\mathbf{r} U(r) e^{-i\mathbf{k}\cdot\mathbf{r}} \\ &= \int_0^\infty dr r U(r) \int_0^{2\pi} d\theta e^{-ikr\cos(\theta)} \\ &= 2\pi \int_0^\infty dr r U(r) J_0(kr), \end{aligned} \tag{2.4}$$

where J_0 is the zeroth-order Bessel function. From the Fourier transform of a two-

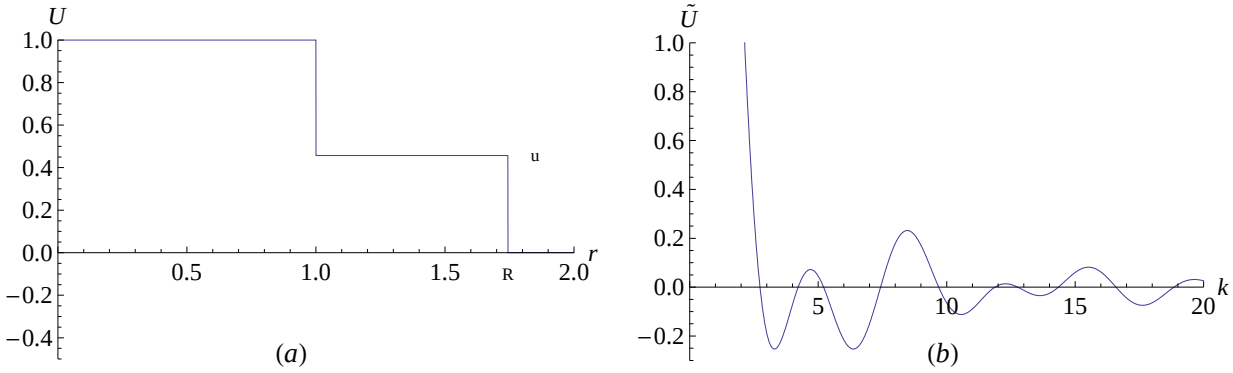

Figure 2.2: Pair potential with a finite core and a soft shoulder in real space (a) where $R = 1.7442$ and $u = 0.457$, and in Fourier space (b) where the ratio between the positions of the two equal-height minima matches 12-fold symmetry ($q \simeq 1.932$), in accordance with Fig. 2.3.

dimensional unit step function

$$\Theta_R(r) = \begin{cases} 1 & 0 < r < R \\ 0 & R < r < \infty, \end{cases} \tag{2.5}$$

that is given by

$$\tilde{\Theta}_R(k) = \frac{2\pi R J_1(kR)}{k}, \tag{2.6}$$

we obtain the Fourier transform of the piecewise constant potential defined in Eq. (2.3), which is given by

$$\tilde{U}(k) = (1-u)\tilde{\Theta}_1(k) + u\tilde{\Theta}_R(k). \tag{2.7}$$

This Fourier transform is plotted in Fig. 2.2(b) for a particular choice of the parameters R and u giving two equal-height minima at wave vectors whose ratio $q \simeq 1.932$ favors the formation of 12-fold structures. Note that $\tilde{U}_{min}$ is negative, as it has to be so that the critical temperature (1.24) is positive. It is also important to note that for the Fourier transform of a single unit step function, *i.e.* a single Bessel function (2.6), the first two minima

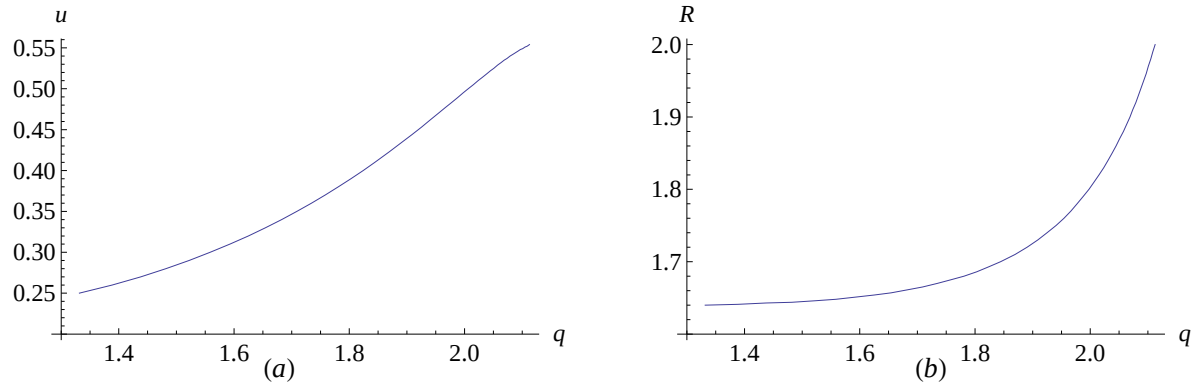

Figure 2.3: The values of the potential parameters (2.3) u (a) and R (b) for a given value of the minima ratio q.

are at different heights with a ratio of approximately 2.2626. This does not comply with the necessary requirements, and so the simple single step core potential cannot stabilize structures with 12-fold symmetries.

We find the minima of the Fourier transformed potential (2.7), by solving the transcendental equation

$$[J_0(k) - J_2(k)]\,\frac{1-u}{4\pi k} + [J_0(kR) - J_2(kR)]\,\frac{R^2 u}{4\pi k} - J_1(k)\frac{1-u}{2\pi k^2} - J_1(kR)\frac{Ru}{2\pi k^2} = 0, \quad (2.8)$$

obtained by setting $d\tilde{U}/dk = 0$. We solve this equation numerically for a range of values of the potential parameters u and R (2.3). We impose the requirement that the two minima be at the same height, and numerically find the values of the potential parameters u and R given any particular value of q—the desired ratio between the positions of the minima. Since we impose two conditions on the potential, we expect to find at most one set of parameters as a solution, and indeed we do find that the ratio q can be selected between 1.3 to 2.1 for a range of the potential parameters, which are plotted in Fig. 2.3.

This demonstrates that even the simplest pair potential with two length scales can be designed to fulfill the requirements needed to stabilize structures with various N-fold sym-

metries, among which is the dodecagonal quasicrystal. However, with two free parameters there is only one solution for any specific ratio between the positions of the two equal-height minima. This is probably why previous studies of a finite core and a soft shoulder potential did not find a quasiperiodic pattern [45–47]. More complicated potentials, with more than two free parameters, may show regions in their parameter space for any desired ratio between the minima. In the next sections we discuss such potentials.

2.2 Pair potential with a van der Waals attraction and a long range repulsion

While a simple Piecewise constant potential as presented in Fig. 2.2 is sufficient for successfully describing the stability of dodecagonal soft quasicrystals, we wish to examine a more realistic interaction. Since the two length scales are a crucial demand, the commonly used Lennard-Jones potential, for example, is not appropriate. It is possible to add more features to the Lennard-Jones potential (see, for example, [16, 25]), but we do not follow this route. Instead, we try to incorporate the most essential elements of the experimental systems [30, 33].

We keep the finite repulsion between overlapping cores of the previous potential (2.3), and replace the uniform shoulder by a van der Waals attraction between two cores and a soft repulsion between overlapping coronas. Denoting r again as the distance between the centers of two micelles, we express this pairwise potential by

$$U(r) = \begin{cases} 1 & 0 < r < 1 \\ -\frac{u_1}{r-1} + u_2 e^{-(r-1)/\lambda} & 1 < r < \infty, \end{cases} \tag{2.9}$$

where the van der Waals term is proportional to $\frac{1}{r-1}$, as appropriate to two spherical

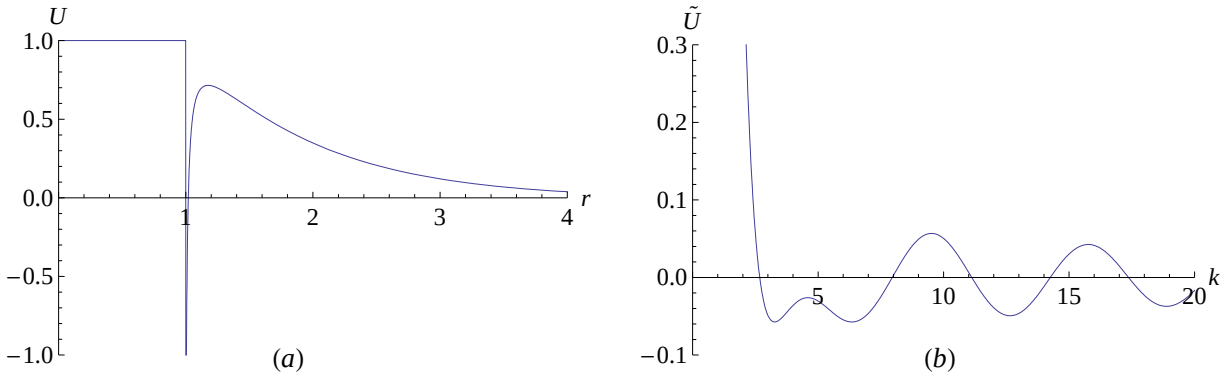

Figure 2.4: Pair potential with a van der Waals attraction and a long range repulsion, as described in Eq. (2.9), as a function of the particle separation in real space (a), where $u_1 = 2.057$, $u_2 = 1.057$ and $\lambda = 0.97561$, and in Fourier space (b), where the first two minima ratio q is 1.932.

surfaces in two dimensions separated by a distance much smaller than their radii ($r-1 \ll 1$) [48]. The soft repulsion length-scale is λ, and its strength is controlled by the parameter u_2. Together with the strength of the van der Waals term controlled by u_1, these three independent parameters control the pair potential.

Fig. 2.4 shows the potential (2.9) for the parameters $u_1 = 2.057$, $u_2 = 1.057$ and $\lambda = 0.97561$. In order to compute the Fourier transform of the infinite van der Waals attraction, we add $\varepsilon = 0.01$ to the denominator. The ratio between the positions of the first two minima, $q \simeq 1.932$, is close to the geometrical value needed to obtain 12-fold symmetry (1.7). In fact, since this pair potential has three independent parameters, all the requirements can be satisfied by a range of parameter values.

2.3 Piecewise constant pair potential—three boxes

We proceed to discuss a simplified potential that includes all the physical phenomena as the previous one (2.9). Using a piecewise constant potential

$$U(r) = \begin{cases} \infty & 0 < r < 1 \\ -u_1 & 1 < r < R_1 \\ u_2 & R_1 < r < R_2 \\ 0 & R_2 < r < \infty, \end{cases} \tag{2.10}$$

we replace the van der Waals interaction with a short range attraction with strength $-u_1$ and width $R_1 - 1$, and replace the exponentially decaying interaction with a uniform repulsion that extends from R_1 to R_2 with strength u_2, as in Fig. 2.5(a).

Using the Fourier transform of a unit step function (2.6), we write the two-dimensional Fourier transform as

$$\tilde{U}(k) = \frac{1+u_1}{k} J_1\left[(1+R_1)k\right] - \frac{u_1+u_2}{k} J_1\left[(R_1+R_2)k\right] + \frac{u_2}{k} J_1(R_2 k). \tag{2.11}$$

We now have four independent parameters u_1, R_1, u_2 and R_2, after having scaled out the dimensions of energy and length, as before. From our discussion of a potential with a hard core and a soft shoulder potential in Sec. 2.1 we learn that two independent parameters give a single solution for any given ratio q. Indeed, for this potential we find a solution within a finite volume in the four-dimensional parameter space, rather then the previous point-like solution described in Sec 2.1. An example to such a solution for a specific set of values of the parameters is plotted in Fig. 2.5(b).

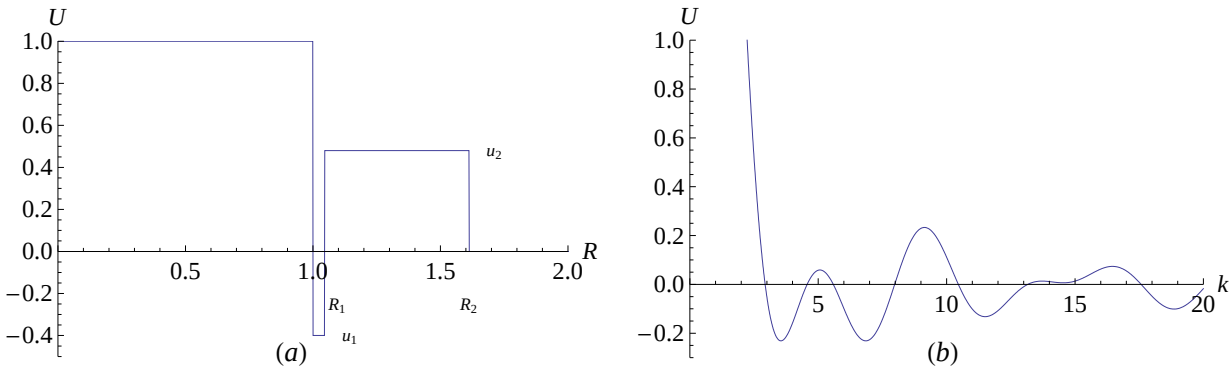

Figure 2.5: Piecewise constant pair potential, as described in Eq. (2.10), as a function of particle separation in real space (a) where $R_1 = 1.04569$, $R_2 = 1.6121$, $u_1 = 0.4$ and $u_2 = 0.48$ so that q, the ratio between the positions of the first two minima in Fourier space (b) is approximately 1.932, very close to the value that prefers the formation of 12-fold symmetry (1.7).

Chapter 3

Free Energy Numerical Calculations

We test our theoretical predictions by finding the minimum of the free energy $\mathcal{F}_{isotropic}$ (1.28) with the pair potentials we discussed. This is done with a numerical solution[1] for the partial differential equation that is related to our free energy via

$$\partial_t \rho = -\frac{\delta \mathcal{F}_{isotropic}\{\rho\}}{\delta \rho}, \tag{3.1}$$

i.e. whose steady-state solution corresponds to minimization of the free-energy functional $\mathcal{F}_{isotropic}\{\rho\}$. Note that this equation does not represent the actual relaxation dynamics because the total density ρ is a conserved order parameter. We use this equation merely to find the minimum of $\mathcal{F}_{isotropic}\{\rho\}$. We calculate the free energy (1.28) by separating the energy and the entropic terms. We use $\tilde{U}(k)$, the full Fourier transform of the pair potential (1.14), instead of its expansion to the series $\{\tilde{a}_{2n}\}$ (1.22), to evaluate the interaction energy in Fourier space, while the entropic contribution expressed in powers of the density ρ is calculated in real space. This numerical calculation starts from a random distribution of the density for a two-dimensional grid containing 256x256 pixels, with periodic boundary conditions. We advance it in time according to Eq. (3.1) until we reach a steady state.

[1] Original code by Michael Cross.

Because our simulation grid is finite, we have to set an upper cutoff for k. Since a high k value in Fourier space refers to a small r value in real space, the value of the Fourier transform of the pair potential $\tilde{U}(k)$ above the cutoff is relevant only for strongly overlapping particles, which is not the case we discuss. For the potentials described in Chapter 2 the two equal-height minima are the global minimum of $\tilde{U}(k)$, and thus determine the steady state solution which is not influenced by the value of the potential for any other k values, in particular for high k values for which $\tilde{U}(k)$ goes to zero.

All the potentials discussed in Chapter 2 are simulated, with the same choice of parameters previously presented, so that the ratio q between the minima is close to the analytical value (1.7) favoring 12-fold patterns. The temperature and density are chosen so that a 12-fold pattern has the lowest free energy, according to our analytical predictions (1.32). The resulting stable patterns, shown in Fig 3.1(c), are the same for all the potentials. It is easy to recognize the dodecagonal symmetry by the 12 Bragg peaks on two different circles in Fourier space. These circles are located at the potential's first two minima in Fourier space. When the temperature and density are chosen so that a 6-fold pattern is stable, we obtain hexagons or compressed hexagons, depending on the initial conditions—see Fig. 3.1(a,b). Setting any one of the potentials so that the ratio q matches 4-fold and 6-fold symmetries, we obtain the tetragonal and hexagonal patterns shown in Fig. 3.2(a,b). The sensitivity of the numerical results to the value of the ratio q was tested using the simple piecewise constant pair potential (2.3). The same steady states were obtain even when the ratio q is shifted from the analytical value (1.7) by about 1%.

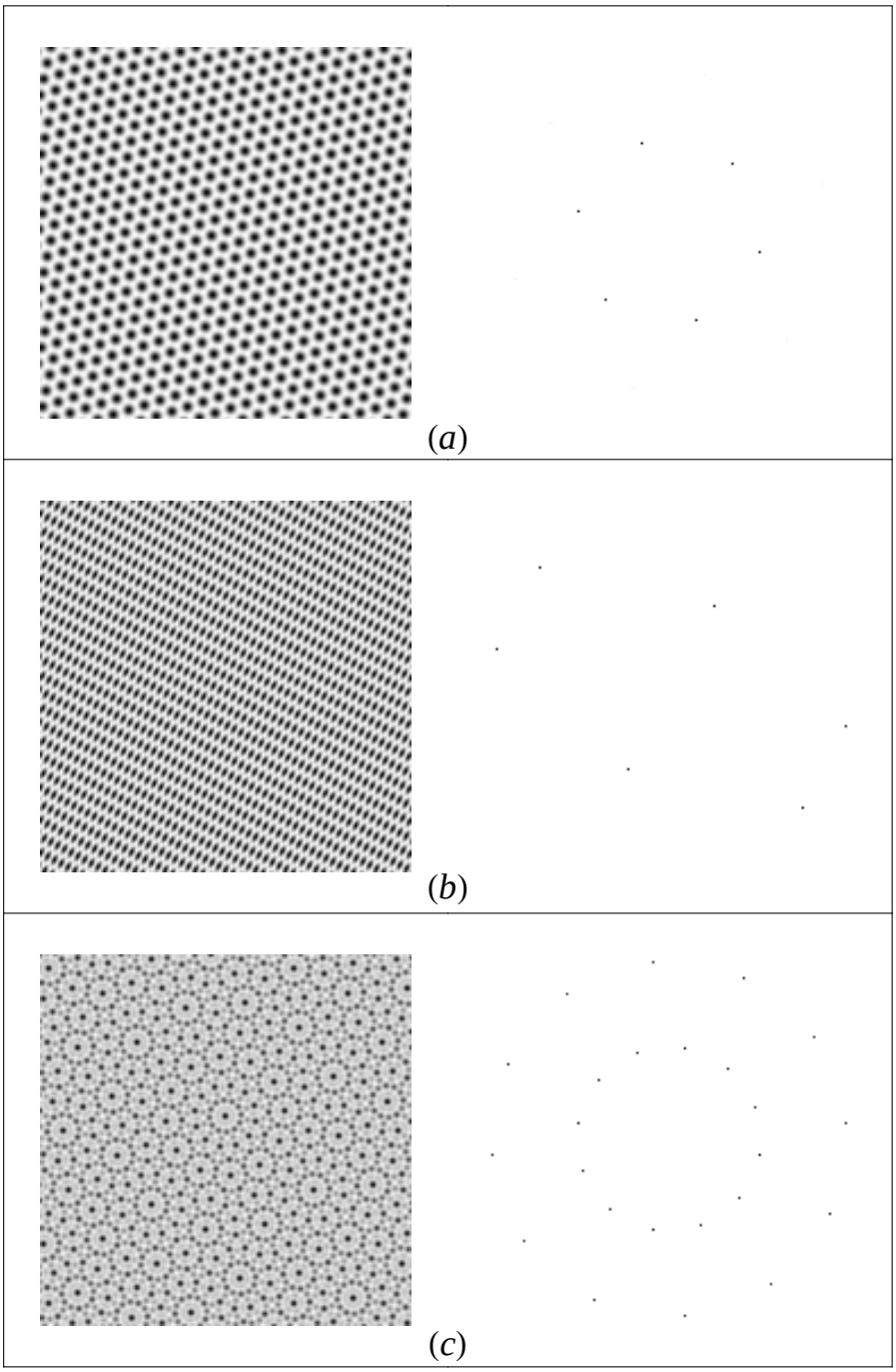

Figure 3.1: Steady state in real space (left) and Fourier space (right). The ratio q between the minima is approximately 1.932 to favor 12-fold pattern. The choice of temperature T and mean density $\bar{c}$ determines the resulting pattern: (a) hexagonal, (b) compressed hexagonal, or (c) dodecagonal.

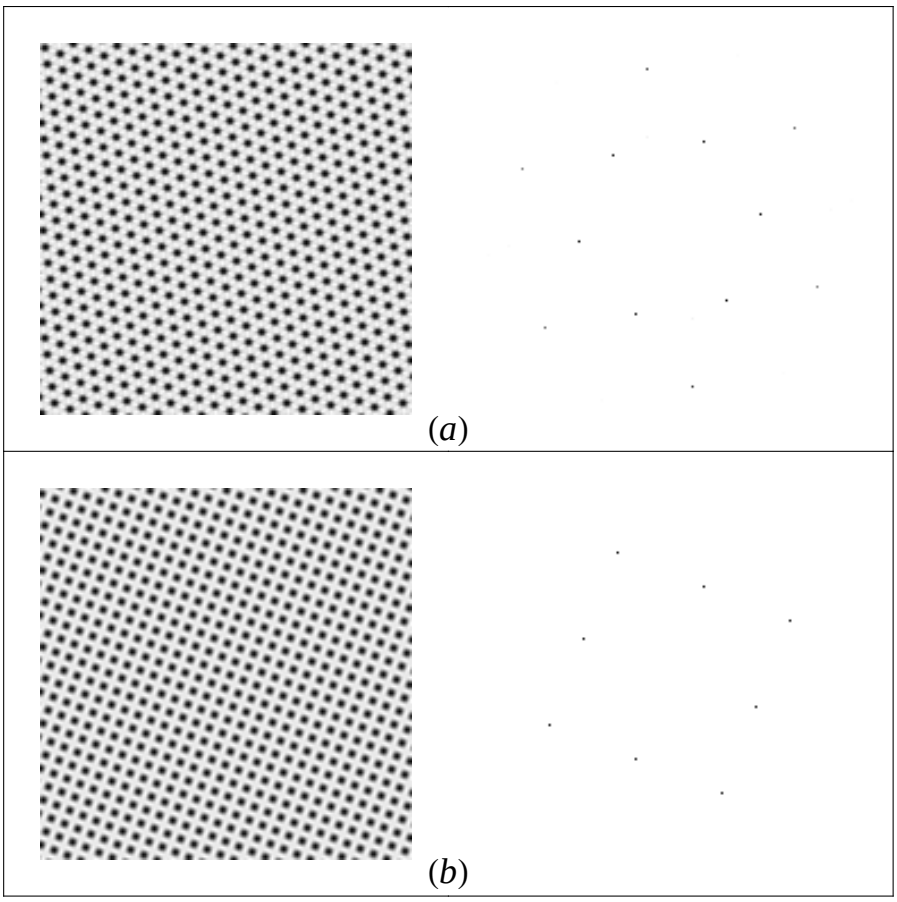

Figure 3.2: Steady state in real space (left) and Fourier space (right). (a) 6-fold superstructure of hexagons is obtained for $q \simeq 1.732$. (b) $q \simeq 1.414$ yields a 4-fold pattern of squares.

Conclusions

In this work we described a new theoretical model for the stability of single-component quasicrystals with isotropic pair-potentials. The model is particularly appropriate for soft-matter systems where density variations occur over length scales much larger than molecular dimensions. We obtained the free energy of a single component two-dimensional liquid characterized by an isotropic pair potential, and the stable symmetries for different values of the macroscopic and microscopic parameters. We discussed several pair potentials that meets the model requirements, and tested them via a numerical simulation that confirmed the validity of the theoretical predictions.

Our model relates the microscopic description of soft materials, via the parameters of the pair potential, to the symmetry formed when they crystalized. 4-fold and 6-fold crystals and 12-fold quasicrystals are predicted, while 8-fold and 10-fold symmetries are not stable, in agreement with current experimental results. In the future, we intend to study the stable structures in three dimensions in a similar fashion.

The mean-field approximation of the free energy (1.13) is sufficient for this work, while the derivation presented in the appendix enables one to go beyond mean-field theory to higher order correlations. Comparing this approximation with LP's free energy functional (1.5), we can discern the roles of energy and entropy in stabilizing the quasiperiodic pattern within our current description. The pairwise interaction yields two length scales, whereas entropy provides an effective three-body interaction term ρ^3. Incorporating actual (rather

than effective) three-body interactions, that may modify this term, is left for a future study.

Previous studies of QCs focused on the interaction potential. The researchers obtained two length scales in real space by assuming various pair potentials such as a Lennard-Jones potential with an additional repulsive maximum [16–21] or attractive minimum [25–28], a hard core potential with a repulsive [23, 24] or attractive shoulder [22], and even more complicated ones [14, 15]. Indeed, these potentials are similar to the potentials discussed in Chapter 2, but, motivated by the LP equation, we looked in Fourier space for the two length scales needed for the description of QCs. We have thus not limited ourselves to any one certain interaction potential and our results are valid as long as the Fourier transform of the pair potential meets the conditions described in Chapter 2. This prediction is confirmed for three different pair potentials that could straightforwardly be designed to stabilize a dodecagonal QC.

Appendix A

Coarse-Grained Free Energy for a System of Pairwise Interacting Particles

We show here how one can coarse-grain a partition function for discrete isotropic particles with pairwise interactions into a free energy functional of a continuous density field. The statistical-mechanical method is standard, and the derivation is general [49]. For our purposes, the mean-field level is satisfactory. However, this systematic derivation enables one to go beyond the mean-field approximation, which may be useful in future studies.

We assume that all the interactions between particles in our system can be described by a translation-invariant, isotropic, pair potential

$$U(\mathbf{r}, \mathbf{r}') = U(|\mathbf{r} - \mathbf{r}'|). \tag{A.1}$$

That is, we assume that interactions between several particles are superpositions of the interactions between pairs of particles. For N particles the Hamiltonian is given by

$$H(N) = \frac{1}{2} \sum_{i \neq j} U(|\mathbf{r}_i - \mathbf{r}_j|), \tag{A.2}$$

where we do not sum over self-interactions. The microscopic density is defined as the sum of delta functions representing the positions of the particles

$$c(\mathbf{r}) = \sum_{i=1}^{N} \delta(\mathbf{r} - \mathbf{r}_i). \tag{A.3}$$

Then, we can rewrite the Hamiltonian of N particles from Eq. (A.2) as an integral over the entire volume V

$$H(N) = \frac{1}{2} \int d\mathbf{r} d\mathbf{r}' c(\mathbf{r}) U(|\mathbf{r} - \mathbf{r}'|) c(\mathbf{r}') - \frac{1}{2} N U(0), \tag{A.4}$$

where we exclude the self-interactions explicitly.

In the canonical ensemble, the partition function of a monatomic fluid is given by

$$\mathcal{Z}_C(N, V, T) = \frac{1}{N! \Lambda^{dN}} \int \prod_{i=1}^{N} d\mathbf{r}_i \exp(-\beta H(N)), \tag{A.5}$$

where $\beta = 1/k_B T$ is the inverse temperature, $\Lambda = h/\sqrt{2\pi m k_B T}$ is the thermal de-Broglie wavelength, and d is the dimensionality (here $d = 2$). We can insert the explicit form of the Hamiltonian of N particles, Eq. (A.4),

$$\mathcal{Z}_C(N, V, T) = \frac{1}{N! \Lambda^{dN}} \int \prod_{i=1}^{N} d\mathbf{r}_i \exp\left[-\frac{\beta}{2} \int d\mathbf{r} d\mathbf{r}' c(\mathbf{r}) U(|\mathbf{r} - \mathbf{r}'|) c(\mathbf{r}') + \frac{\beta}{2} N U(0) \right], \tag{A.6}$$

and separate the self-interaction term

$$\begin{aligned} \mathcal{Z}_C(N, V, T) &= \frac{1}{N! \Lambda^{dN}} \exp\left(\frac{\beta U(0)}{2} N \right) \int \prod_{i=1}^{N} d\mathbf{r}_i \exp\left[-\frac{\beta}{2} \int d\mathbf{r} d\mathbf{r}' c(\mathbf{r}) U(|\mathbf{r} - \mathbf{r}'|) c(\mathbf{r}') \right] \\ &= \frac{Z_0^N}{N!} \int \prod_{i=1}^{N} d\mathbf{r}_i e^{-\beta H}, \end{aligned} \tag{A.7}$$

where we denote $Z_0 = e^{\beta U(0)/2}/\Lambda^d$, and

$$H = \frac{1}{2}\int d\mathbf{r}d\mathbf{r}' c(\mathbf{r})U(|\mathbf{r}-\mathbf{r}'|)c(\mathbf{r}'), \tag{A.8}$$

is the pairwise-interaction Hamiltonian of the continuous density.

Using the chemical potential μ, we write the partition function in the grand canonical ensemble

$$\mathcal{Z}_{GC}(\mu,V,T) = \sum_{N=0}^{\infty} e^{\beta\mu N}\mathcal{Z}_C(N,V,T) = \sum_{N=0}^{\infty}\frac{Z_0^N\zeta^N}{N!}\int\prod_{i=1}^{N}d\mathbf{r}_i\exp(-\beta H), \tag{A.9}$$

where $\zeta = e^{\beta\mu}$ is the fugacity. We substitute the density (A.3) into the Hamiltonian (A.8) by making use of a delta function in the expression (A.9) of $\mathcal{Z}_{GC}$ and obtain a functional integration over the density,

$$\mathcal{Z}_{GC} = \sum_{N=0}^{\infty}\frac{Z_0^N\zeta^N}{N!}\int\mathcal{D}c(\mathbf{r})\int\prod_{i=1}^{N}d\mathbf{r}_i\delta\left(c(\mathbf{r}) - \sum_{j=1}^{N}\delta(\mathbf{r}-\mathbf{r}_j)\right)\exp(-\beta H). \tag{A.10}$$

We represent the delta function using a field $\psi(\mathbf{r})$ conjugate to the density

$$\delta\left(c(\mathbf{r}) - \sum_{j=1}^{N}\delta(\mathbf{r}-\mathbf{r}_j)\right) = \int\mathcal{D}\psi(\mathbf{r})\exp\left[i\int d\mathbf{r}\psi(\mathbf{r})\left(c(\mathbf{r}) - \sum_{j=1}^{N}\delta(\mathbf{r}-\mathbf{r}_j)\right)\right], \tag{A.11}$$

and substitute this representation into the partition function (A.10)

$$\begin{aligned}\mathcal{Z}_{GC} &= \sum_{N=0}^{\infty} \frac{Z_0^N \zeta^N}{N!} \int \mathcal{D}c(\mathbf{r})\mathcal{D}\psi(\mathbf{r}) \\ &\qquad \int \prod_{i=1}^{N} d\mathbf{r}_i \exp\left[-\beta H + i\int d\mathbf{r}\psi(\mathbf{r})\left(c(\mathbf{r}) - \sum_{j=1}^{N}\delta(\mathbf{r}-\mathbf{r}_j)\right)\right] \\ &= \int \mathcal{D}c(\mathbf{r})\mathcal{D}\psi(\mathbf{r}) \exp\left[-\beta H + i\int d\mathbf{r}\psi(\mathbf{r})c(\mathbf{r})\right] \\ &\qquad \sum_{N=0}^{\infty} \frac{Z_0^N \zeta^N}{N!} \int \prod_{i=1}^{N} d\mathbf{r}_i \exp\left[-i\sum_{j=1}^{N}\psi(\mathbf{r}_j)\right]. \end{aligned} \tag{A.12}$$

We notice that the last term is the product of N identical integrals, and so we have

$$\mathcal{Z}_{GC} = \int \mathcal{D}c(\mathbf{r})\mathcal{D}\psi(\mathbf{r}) \exp\left[-\beta H + i\int d\mathbf{r}\psi(\mathbf{r})c(\mathbf{r})\right] \sum_{N=0}^{\infty} \frac{Z_0^N \zeta^N}{N!} \left(\int d\mathbf{r} e^{-i\psi(\mathbf{r})}\right)^N. \tag{A.13}$$

We identify the formal representation of the exponent function

$$e^x = \sum_{N=0}^{\infty} \frac{x^N}{N!}, \tag{A.14}$$

and obtain the partition function

$$\mathcal{Z}_{GC} = \int \mathcal{D}c(\mathbf{r})\mathcal{D}\psi(\mathbf{r}) \exp\left[-\beta H + i\int d\mathbf{r}\psi(\mathbf{r})c(\mathbf{r}) + Z_0\zeta\int d\mathbf{r} e^{-i\psi(\mathbf{r})}\right]. \tag{A.15}$$

This partition function is exactly equal to the one we started with, Eq. (A.9), yet now it is expressed in terms of the continuous fields $c(\mathbf{r})$ and $\psi(\mathbf{r})$, rather than the discrete particle positions $\mathbf{r}_j$.

We perform the integration over ψ

$$I_\psi = \int \mathcal{D}\psi(\mathbf{r}) \exp\left[\int d\mathbf{r}\left(i\psi(\mathbf{r})c(\mathbf{r}) + Z_0\zeta e^{-i\psi(\mathbf{r})}\right)\right], \tag{A.16}$$

using a saddle point approximation. That is, we replace the integrand $f(\psi) = i\psi c + Z_0\zeta e^{-i\psi}$ with its extremal value. The field $\bar{\psi}$ that gives an extremum for the integrand is given by

$$\frac{\partial f(\psi)}{\partial \psi} = 0 \qquad \Rightarrow \qquad \bar{\psi} = i \ln \frac{c}{Z_0 \zeta}. \tag{A.17}$$

So the extremal value of the integrand $f(\psi)$ is

$$f(\bar{\psi}) = c - c \ln \frac{c}{Z_0 \zeta}. \tag{A.18}$$

Note that this formalism can be extended to higher order approximations, but for our purposes we need only the first order that can be shown to be equivalent to a mean-field approximation. Within this saddle-point approximation we thus obtain

$$I_\psi = \exp\left[\int d\mathbf{r} \left(c(\mathbf{r}) - c(\mathbf{r}) \ln \frac{c(\mathbf{r})}{Z_0 \zeta} \right)\right]. \tag{A.19}$$

Substituting I_ψ into the partition function (A.15), we obtain

$$\mathcal{Z}_{GC} \simeq \int \mathcal{D}c(\mathbf{r}) \exp\left[-\beta H + \int d\mathbf{r} \left(c(\mathbf{r}) - c(\mathbf{r}) \ln \frac{c(\mathbf{r})}{Z_0 \zeta} \right)\right]. \tag{A.20}$$

Upon substitution of the expression for the Hamiltonian (A.8), we obtain the main result of the Appendix—the free energy of a system described by pairwise interactions

$$\mathcal{F} = \frac{1}{2} \int d\mathbf{r} d\mathbf{r}' c(\mathbf{r}) U(|\mathbf{r} - \mathbf{r}'|) c(\mathbf{r}') + k_B T \int d\mathbf{r} \left(c(\mathbf{r}) \ln \frac{c(\mathbf{r})}{Z_0 \zeta} - c(\mathbf{r}) \right). \tag{A.21}$$

Note that Eq. (A.21) is the familiar mean-field free energy, containing ideal entropy and pair interactions, and could have been written down at the outset. The advantage of the rigorous formulation presented here is that it provides this familiar result as the leading order in a systematic expansion, which can be improved further if needed.

Bibliography

[1] J.W. Cahn. Epilogue. In C. Janot and R. Mosseri, editors, *Proceedings of the 5th International Conference on Quasicrystals*, volume 807. World Scientific, Singapore, 1996.

[2] D. Shechtman, I. Blech, D. Gratias, and J. W. Cahn. Metallic phase with long-range orientational oreder and no translational symmetry. *Phys. Rev. Lett.*, 53:1951–1953, 1984.

[3] D. Levine and P.J. Steinhardt. Quasicrystals: A new class of ordered structures. *Phys. Rev. Lett.*, 53:2477–2480, 1984.

[4] W. Steurer and S. Deloudi. Fascinating quasicrystals. *Acta Crystallograohica*, A64:1–11, 2007.

[5] A.-P. Tsai. Icosahedral clusters, icosaheral order and stability of quasicrystals - a view of metallurgy. *Science and Technology of Advanced Materials*, 9:013008, 2008.

[6] I.R. Fisher, Z. Islam, A.F. Panchula, K.O. Cheon, M.J. Kramer, P.C., Canfield, and A.I. Goldman. Growth of large-grain R-Mg-Zn quasicrystals from the ternary melt (R = Y, Er, Ho, Dy and Tb). *Phil. Mag. B*, 77:1601–1615, 1998.

[7] R. Lifshitz. Quasicrystals: A matter of definition. *Found. Phys.*, 43:1703–1711, 1991.

[8] C. Janot. *Quasicrystals: A Primer*. Calderon Press, Oxford, 2nd edition, 1994.

[9] D. Levine and P.J. Steinhardt. Quasicrystals. I. defintion and structure. *Phys. Rev. B*, 34:596–616, 1986.

[10] M. Senechal. *Quasicrystals and geometry*. Cambridge University Press, Cambridge, 1995.

[11] International Union of Crystallography. *Acta Cryst. A*, 48:922, 1992.

[12] M. de Boissieu. Stability of quasicrystals: energy, entropy and phason modes. *Phil. Mag.*, 86:1115–1122, 2006.

[13] M. Widom. Discussion of phasons in quasicrystals and their dynamics. *Phil. Mag.*, 88:2339–2350, 2008.

[14] Z. Olami. Stable dense icosahedral quasicrystals. *Phys. Rev. Lett.*, 65:2559–2562, 1990.

[15] A.P. Smith. Stable one-component quasicrystals. *Phys. Rev. B*, 43:11635–11641, 1991.

[16] M. Dzugutov and U. Dahlborg. Molecular dynamics study of the coherent density correlation function in a supercooled simple one-component liquid. *Journal of Non-Crystalline Solids*, 131:62–65, 1991.

[17] M. Dzugutov. Formation of a dodecagonal quasicrystalline phase in a simple monatomic liquid. *Phys. Rev. Lett.*, 70:2924–2927, 1993.

[18] M. Dzugutov. Glass formation in a simple monatomic liquid with icosahedral inherent local order. *Physical Review A*, 46:R2984–R2987, 1992.

[19] A. Quandt and M.P. Teter. Formation of quasiperiodic patterns within a simple two-dimensional model system. *Phys. Rev. B*, 59:8586–8592, 1999.

[20] J. Roth and A.R. Denton. Solid-phase structures of the Dzugutov pair potential. *Physical Review E*, 61:6845–6857, 2000.

[21] A.S. Keys and S.C. Glotzer. How do quasicrystals grow? *Phys. Rev. Lett.*, 99:235503, 2007.

[22] A. Skibinsky, S.V. Buldyrev, A. Scala, S. Havlin, and H.E. Stanley. Quasicrystals in a monodisperse system. *Phys. Rev. E*, 60:2664–2669, 1999.

[23] E. A. Jagla. Phase behavior of a system of particles with core collapse. *Physical Review E*, 58:1478–1486, 1998.

[24] E. A. Jagla. Minimum energy configurations of repelling particles in two dimensions. *Journal of Chemical Physics*, 110:451–456, 1999.

[25] M. Engel and H.-R. Trebin. Self-assembly of monatomic complex crystals and quasicrystals with a double-well interaction potential. *Phys. Rev. Lett.*, 98:225505, 2007.

[26] M. Engel and H.-R. Trebin. Structural complexity in monodisperse systems of isotropic particles. *Z. Kristallogr.*, 223:721–725, 2008.

[27] M. Engel and H.-R. Trebin. Stability of the decagonal quasicrystal in the Lennard-Jones-Gauss system. *Philosophical Magazine*, 88:1959–1965, 2008.

[28] V. Van Hoang and T. Odagaki. Glasses of simple liquids with double-well interaction potential. *Physica B*, 403:3910–3915, 2008.

[29] P.-G. de Gennes and J. Prost. *The Physics of Liquid Crystals*. Oxford University Press, New York, 2nd edition, 1993.

[30] X.B. Zeng, G. Unger, Y. Liu, V. Percec, A. E. Dulcey, and J. K. Hobbs. Supramolecular dendritic liquid quasicrystals. *Nature*, 428:157–160, 2004.

[31] G. Ungar and X.B. Zeng. Frank-Kasper, quasicrystalline and related phases in liquid crystals. *Soft Matter*, 1:95–106, 2005.

[32] X.B. Zeng. Liquid quasicrystals. *Current Opinion in Colloid and Interface Science*, 9:384–389, 2005.

[33] K. Hayashida, T. Dotera, A. Takano, and Y. Matsushita. Polymeric quasicrystal: Mesoscopic quasicrystalline tiling in ABC star polymers. *Phys. Rev. Lett.*, 98:195502, 2007.

[34] A. Takano, S. Wada, S. Sato, T.Araki, K. Hirahara, T. Kazama, S. Kawahara, Y. Isono, A. Ohno, N. Tanaka, and Y. Matsushita. Observation of cylinder-based microphase-separated structures from ABC star-shaped terpolymers investigated by electron computerized tomography. *Macromolecules*, 37:9941–9946, 2004.

[35] V. Percec, M.R. Imam, D.A. Wilson, W Graf, H.W. Spiess, V.S.K. Balagurusamy, and P.A. Heiney. Self-assembly of dendronized triphenylenes into helical pyramidal columns and chiral spheres. *J. Am. Chem. Soc.*, 131:7662–7677, 2009.

[36] T.A. Witten. *Structured Fluids*. Oxford University Press, Oxford, 2004.

[37] C. Tschierske. Liquid crystal engineering - new complex mesophase structures and their relations to polymer morphologies, nanoscale patterning and crystal engineering. *Chemical Society Reviews*, 36:1930–1970, 2007.

[38] T. Dotera. Mean-field theory of archimedean and quasicrystalline tilings. *Phil. Mag.*, 87:3011–3019, 2007.

[39] R. Lifshitz and D. M. Petrich. Theoretical model for Faraday waves with multiple-frequency forcing. *Phys. Rev. Lett.*, 79:1261–1264, 1997.

[40] W.S. Edwards and S. Fauve. Parametrically excited quasicrystalline surface waves. *Phys. Rev. E*, 47:R788–R791, 1993.

[41] A. Kudrolli, B. Pier, and J. P. Gollub. Superlattice patterns in surface waves. *Phys. D*, 123(1-4):99–111, 1998.

[42] H. Arbell and J. Fineberg. Pattern formation in two-frequency forced parametric waves. *Phys. Rev. E*, 65(3):036224, 2002.

[43] R. Lifshitz and H. Diamant. Soft quasicrystals − why are they stable?. *Philosophical Magazine*, 87:3021–3030, 2007.

[44] J. B. Swift and P. C. Hohenberg. Hydrodynamic fluctuations at the convective instability. *Phys. Rev. A*, 15:319, 1977.

[45] G. Malescio and G. Pellicane. Stripe phases from isotropic repulsive interactions. *Nature Materials*, 2:97–100, 2003.

[46] M. A. Glaser, G. M. Grason, R. D. Kamien, A. Košmrlj, C. D. Santangelo, and P. Ziherl. Soft spheres make more mesophases. *Europhysics Letters*, 78:46004–46007, 2007.

[47] N. B. Wilding and J. E. Magee. Phase behavior and thermodynamic anomalies of core-softened fluids. *Physical Review E*, 66:031509, 2002.

[48] J.N. Israelachvili. *Intermolecular and Surface Forces*. Academic Press, 2nd edition, 1991.

[49] G.H. Fredrickson. *The Equilibrium Theory of Inhomogeneous Polymers*. Oxford University Press, Oxford, 2006.